

PATHWISE MIMO CHANNEL MODELING AND ESTIMATION

Maxime Guillaud

Dirk T.M. Slock

Eurecom Institute

Eurecom Institute

2229 route des Crêtes, B.P. 193

2229 route des Crêtes, B.P. 193

06904 Sophia Antipolis Cedex, FRANCE

06904 Sophia Antipolis Cedex, FRANCE

Tel: +33 4 9300 2647; Fax: +33 4 9300 2627

Tel: +33 4 9300 2606; Fax: +33 4 9300 2627

maxime.guillaud@eurecom.fr

dirk.slock@eurecom.fr

ABSTRACT

A specular approach to time-varying frequency-selective MIMO channel modeling is proposed, that yields a parsimonious channel representation. Essentially, the vector of channel impulse response coefficients lives in a subspace that is subject to slow fading and hence is time-invariant over a reasonable time interval. The subspace is parameterized by the (deterministic) slow path parameters, that may comprise path delay, angle of departure and angle of arrival. The channel expansion into this propagation signature subspace yields coefficients that are subject to fast fading. They are modeled as independent lowpass autoregressive processes. We present an analysis of the identifiability of specular channels, and an algorithm achieving identification, as well as a performance evaluation over actual channel measurements.

1. INTRODUCTION

The use of specular models for wireless channel analysis and tracking has been proposed by various authors seeking to improve the ability to accurately estimate [1] or predict [2, 3] the channel state. Specular methods constitute viable candidates for channel tracking and prediction, since the insight they provide into the actual channel structure – namely, separation of the channel variation into its space and time components – can improve the performance and decrease the complexity of channel tracking and prediction. Various methods have been proposed to estimate the underlying parameters, including MUSIC [2], ESPRIT [3] and SAGE [1].

This paper is a follow-up to [4], with added experimental results. We propose to use a specular (pathwise) approach in order to gain access to a reduced parameter set representing the channel state, in order to improve channel estimation (smoothing) and prediction. After recalling the specular channel model in section 2, and outlining in section 3 how it makes channel estimation and prediction eas-

ier, we provide sufficient conditions for identifiability of a specular channel in section 4, and an algorithm, based on simultaneous diagonalization of the covariance matrices, that achieves identification is proposed in section 5. Section 6 presents experimental results.

2. SPECULAR CHANNEL MODEL

Let us consider a Multiple-Input Multiple-Output (MIMO) frequency-selective channel, with N_t transmit (Tx) and N_r receive (Rx) antennas. The impulse response of the channel between the i^{th} Tx antenna and the j^{th} Rx antenna is denoted by $h_{i,j}(t, \tau)$, where t is the time and τ is the lag. We will henceforth work under the assumption that the channel state evolves according to a specular model. In such a model, each impulse response $h_{i,j}(t, \cdot)$ is the superposition of a finite number P of discrete paths at lag $\tau_p^{(i,j)} = l_p^{(i,j)} T_s$, $p = 1 \dots P$, resulting from either line-of-sight propagation, or one or several reflections. This model relies upon the fact that the paths between all the Tx-Rx antenna pairs have most of their characteristics in common, except for what happens near the antenna arrays. Hence, they share some properties, namely their speed w.r.t. the reflectors, and the reflection characteristics (hence their Doppler and gain are the same whatever antenna pair is considered). Each path coefficient can be decomposed into a product of two components:

- a space component $\alpha_p^{(i,j)}$, which depends on the physical properties of path p between Tx antenna i and Rx antenna j , including antennas and reflectors position, path loss, etc.
- a time component $\beta_p(t)$ which includes the Doppler due to reflectors motion and the relative speed of the transmitter w.r.t. the receiver.

The time components $\beta_p(t)$ are assumed to be independent between paths, hence $p \neq p' \Rightarrow \mathcal{E}_n[\beta_p(t) \beta_{p'}(t')] = 0 \quad \forall(t, t')$. Note that we consider a time scale where they

evolve significantly during time, *e.g.* due to the Doppler effect, and hence can be considered random processes, whereas the physical properties of the problem, comprised of the $\alpha_p^{(i,j)}$, do not vary. In discrete time, the specular channel model yields

$$h_{n,l}^{(i,j)} \triangleq h_{i,j}(nT_s, lT_s) = \sum_{p=1}^{P^{(i,j)}} \alpha_p^{(i,j)} \beta_{n,p} \delta_{l_p^{(i,j)}}(l), \quad (1)$$

where we used the discretized version of the time component $\beta_{n,p} \triangleq \beta_p(nT_s)$ where T_s is the sampling interval at the receiver. Let us assume that the impulse response has finite support, and consider its discretized version

$$\underline{\mathbf{h}}_n^{(i,j)} \triangleq [h_{n,0}^{(i,j)}, \dots, h_{n,L-1}^{(i,j)}]^T, \quad (2)$$

with L chosen such that all the channel coefficients outside the lag interval $[0 \dots (L-1)T_s]$ are zero. Let us further stack these into a row vector with $N_t N_r L$ coefficients $\underline{\mathbf{h}}_n \triangleq [\underline{\mathbf{h}}_n^{(1,1)T} \dots \underline{\mathbf{h}}_n^{(1,N_r)T}, \underline{\mathbf{h}}_n^{(2,1)T} \dots \underline{\mathbf{h}}_n^{(N_t, N_r)T}]^T$. We emphasize the fact that $\underline{\mathbf{h}}_n$ constitutes a snapshot of all the channel impulse response coefficients at time nT_s . With this notation, (1) can be rewritten in more compact form as

$$\underline{\mathbf{h}}_n = \mathbf{G} \underline{\mathbf{b}}_n \quad (3)$$

where $\underline{\mathbf{a}}_p^{(i,j)} \triangleq \alpha_p^{(i,j)} (\delta_{l_p^{(i,j)}}(0) \dots \delta_{l_p^{(i,j)}}(L-1))$, $\underline{\mathbf{a}}_p \triangleq (\underline{\mathbf{a}}_p^{(1,1)} \dots \underline{\mathbf{a}}_p^{(1,N_r)}, \underline{\mathbf{a}}_p^{(2,1)} \dots \underline{\mathbf{a}}_p^{(N_t, N_r)})^T$, $\mathbf{G} \triangleq [\underline{\mathbf{a}}_1, \dots, \underline{\mathbf{a}}_P]$, and $\underline{\mathbf{b}}_n \triangleq (\beta_{n,1}, \dots, \beta_{n,P})^T$.

3. SPECTRAL FACTORIZATION AND LINEAR ESTIMATION

In this section, we outline the possible improvements in channel tracking that can be achieved by deconstructing a specular channel, *i.e.* by separating the time and space properties as enounced in the previous section before doing any kind of smoothing or prediction. We seek to model the discrete-time random process $\{\underline{\mathbf{h}}_n\}$ from its noisy measurements $\tilde{\underline{\mathbf{h}}}_n = \underline{\mathbf{h}}_n + \underline{\mathbf{v}}_n$ where the noise $\{\underline{\mathbf{v}}_n\}$ is white Gaussian, *i.i.d.*, independent from $\{\underline{\mathbf{h}}_n\}$. Assuming that both $\{\underline{\mathbf{h}}_n\}$ and $\{\underline{\mathbf{v}}_n\}$ are wide-sense stationary (WSS), let us define the (matrix) covariances $\mathbf{R}_{\tilde{\underline{\mathbf{h}}}\tilde{\underline{\mathbf{h}}}}(u) \triangleq \mathcal{E}_n[\tilde{\underline{\mathbf{h}}}_{n+u} \tilde{\underline{\mathbf{h}}}_n^H]$ and $\mathbf{R}_{\underline{\mathbf{h}}\underline{\mathbf{h}}}(u) \triangleq \mathcal{E}_n[\underline{\mathbf{h}}_{n+u} \underline{\mathbf{h}}_n^H]$, where $\mathcal{E}_n[\cdot]$ is the expectation operator taken over n , and the z -transforms

$$\begin{aligned} \mathbf{S}_{\tilde{\underline{\mathbf{h}}}\tilde{\underline{\mathbf{h}}}}(z) &\triangleq \sum_{u=-\infty}^{+\infty} \mathbf{R}_{\tilde{\underline{\mathbf{h}}}\tilde{\underline{\mathbf{h}}}}(u) z^{-u} \quad \text{and} \\ \mathbf{S}_{\underline{\mathbf{h}}\underline{\mathbf{h}}}(z) &\triangleq \sum_{u=-\infty}^{+\infty} \mathbf{R}_{\underline{\mathbf{h}}\underline{\mathbf{h}}}(u) z^{-u}. \end{aligned} \quad (4)$$

Note that due to the independence between $\{\underline{\mathbf{v}}_n\}$ and $\{\underline{\mathbf{h}}_n\}$, $\mathbf{S}_{\tilde{\underline{\mathbf{h}}}\tilde{\underline{\mathbf{h}}}}(z) = \mathbf{S}_{\underline{\mathbf{h}}\underline{\mathbf{h}}}(z)$ and $\mathbf{S}_{\tilde{\underline{\mathbf{h}}}\tilde{\underline{\mathbf{h}}}}(z) = \mathbf{S}_{\underline{\mathbf{h}}\underline{\mathbf{h}}}(z) + \mathbf{S}_{\underline{\mathbf{v}}\underline{\mathbf{v}}}(z)$.

Spectral factorization of $\mathbf{S}_{\tilde{\underline{\mathbf{h}}}\tilde{\underline{\mathbf{h}}}}(z)$, of the form

$$\mathbf{S}_{\tilde{\underline{\mathbf{h}}}\tilde{\underline{\mathbf{h}}}}(z) = \mathbf{L}(z) \mathbf{R}_e \mathbf{L}^*(z^{-*}), \quad (5)$$

is desirable, since the best linear estimator (in terms of mean square error) of $\underline{\mathbf{h}}_{n+\lambda}$, $\lambda \geq 0$ given $\{\underline{\mathbf{h}}_k\}_{k=-\infty}^n$ is defined through its z -transform by [5]

$$\mathbf{K}(z) = \left\{ z^\lambda \mathbf{S}_{\tilde{\underline{\mathbf{h}}}\tilde{\underline{\mathbf{h}}}}(z) \mathbf{L}^{-*}(z^{-*}) \right\}_+ \mathbf{R}_e^{-1} \mathbf{L}^{-1}(z). \quad (6)$$

In general, spectral factorization is hard to compute in the case of vector-valued processes, and (6) is not feasible.

3.1. Specular model and spectral factorization

Under the assumption that the channel variations follow the specular model (3), the covariances become

$$\mathbf{R}_{\tilde{\underline{\mathbf{h}}}\tilde{\underline{\mathbf{h}}}}(u) = \mathbf{G} \mathcal{E}_n[\underline{\mathbf{b}}_{n+u} \underline{\mathbf{b}}_n^H] \mathbf{G}^H + \mathcal{E}_n[\underline{\mathbf{v}}_{n+u} \underline{\mathbf{v}}_n^H] \quad (7)$$

$$= \mathbf{G} \mathbf{R}_{\underline{\mathbf{b}}\underline{\mathbf{b}}}(u) \mathbf{G}^H + \mathbf{R}_{\underline{\mathbf{v}}\underline{\mathbf{v}}}(u), \quad (8)$$

$$\mathbf{R}_{\underline{\mathbf{h}}\underline{\mathbf{h}}}(u) = \mathbf{G} \mathcal{E}_n[\underline{\mathbf{b}}_{n+u} \underline{\mathbf{b}}_n^H] \mathbf{G}^H = \mathbf{G} \mathbf{R}_{\underline{\mathbf{b}}\underline{\mathbf{b}}}(u) \mathbf{G}^H. \quad (9)$$

Note that in eqs. (7) and (9) the factor \mathbf{G} is independent of the lag u . Therefore, the z -transforms can be factored as

$$\mathbf{S}_{\tilde{\underline{\mathbf{h}}}\tilde{\underline{\mathbf{h}}}}(z) = \mathbf{G} \mathbf{S}_{\underline{\mathbf{b}}\underline{\mathbf{b}}}(z) \mathbf{G}^H + \mathbf{S}_{\underline{\mathbf{v}}\underline{\mathbf{v}}}(z) \quad \text{and} \quad (10)$$

$$\mathbf{S}_{\underline{\mathbf{h}}\underline{\mathbf{h}}}(z) = \mathbf{G} \mathbf{S}_{\underline{\mathbf{b}}\underline{\mathbf{b}}}(z) \mathbf{G}^H. \quad (11)$$

Note that $\mathbf{S}_{\underline{\mathbf{b}}\underline{\mathbf{b}}}(z)$ is diagonal, since we assume that the $\beta_p(t)$ are independent. Therefore, let us denote $\mathbf{S}_{\underline{\mathbf{b}}\underline{\mathbf{b}}}(z) = \text{diag}(s_{bb}^{(1)}(z), \dots, s_{bb}^{(P)}(z))$, where

$$s_{bb}^{(p)}(z) \triangleq \sum_{u=-\infty}^{+\infty} \mathcal{E}_n[\beta_{n+u,p} \beta_{n,p}^*] z^{-u} \quad \text{for } p = 1 \dots P. \quad (12)$$

This structure allows to obtain the spectral factorization of $\mathbf{S}_{\tilde{\underline{\mathbf{h}}}\tilde{\underline{\mathbf{h}}}}(z)$ by performing P independent, scalar spectral factorizations of the $s_{bb}^{(p)}(z)$ (equivalently, this means that the random process $\{\underline{\mathbf{h}}_n\}$ can be accurately tracked by tracking P scalar processes).

In the following sections, we will address the following identifiability problem: assuming the knowledge of the spectrum $\mathbf{S}_{\tilde{\underline{\mathbf{h}}}\tilde{\underline{\mathbf{h}}}}(z)$, we show that if the $s_{bb}^{(p)}(z)$ are linearly independent polynomials, it is possible to identify them up to a permutation and a complex scalar coefficient. Fortunately, this is sufficient for our needs, since all possible solutions yield the same predictor $\mathbf{K}(z)$. We subsequently derive an algorithm that achieves identification.

4. IDENTIFIABILITY

In this section, we show that Let us assume that \mathbf{G} has full column rank, and let $(\underline{\mathbf{c}}_1, \dots, \underline{\mathbf{c}}_P)$ be an orthonormal base of the column subspace of \mathbf{G} . Let $\mathbf{C} \triangleq [\underline{\mathbf{c}}_1, \dots, \underline{\mathbf{c}}_P]$. Let \mathbf{R} denote the representation of \mathbf{G} in this base, such that $\mathbf{G} = \mathbf{C}\mathbf{R}$. Let us assume that $S_{\underline{\mathbf{h}}\underline{\mathbf{h}}}(z)$ has an alternative factorization $S_{\underline{\mathbf{h}}\underline{\mathbf{h}}}(z) = \mathbf{H}\mathbf{S}_{\underline{\mathbf{b}}'\underline{\mathbf{b}}'}(z)\mathbf{H}^H$, and show that \mathbf{G} and \mathbf{H} are identical up to a permutation and a linear scaling of their columns. Using the fact that $\mathbf{C}^H\mathbf{C} = \mathbf{I}_P$, the decomposition in (11) yields $S_{\underline{\mathbf{b}}\underline{\mathbf{b}}}(z) = \mathbf{R}^{-1}\mathbf{C}^H S_{\underline{\mathbf{h}}\underline{\mathbf{h}}}(z)\mathbf{C}\mathbf{R}^{-H}$.

Hence, defining the $P \times P$ matrix $\mathbf{S} \triangleq \mathbf{R}^{-1}\mathbf{C}^H\mathbf{H}$, $S_{\underline{\mathbf{b}}\underline{\mathbf{b}}}(z) = \mathbf{S}\mathbf{S}_{\underline{\mathbf{b}}'\underline{\mathbf{b}}'}(z)\mathbf{S}^H$. Therefore we need to prove that \mathbf{S} is the product of a permutation matrix and a diagonal matrix. Let $\underline{\mathbf{s}}_i, i = 1 \dots P$ denote the columns of \mathbf{S} . The diagonal structure of $S_{\underline{\mathbf{b}}'\underline{\mathbf{b}}'}(z)$ yields $S_{\underline{\mathbf{b}}\underline{\mathbf{b}}}(z) = \sum_{i=1}^P \underline{\mathbf{s}}_i \mathbf{S}_{\underline{\mathbf{b}}'\underline{\mathbf{b}}'}^{(i)}(z) \underline{\mathbf{s}}_i^H$. This implies that each $\underline{\mathbf{s}}_i \mathbf{S}_{\underline{\mathbf{b}}'\underline{\mathbf{b}}'}^{(i)}$ is diagonal, otherwise the off-diagonal terms would yield an identically zero linear combination of $S_{\underline{\mathbf{b}}'\underline{\mathbf{b}}'}^{(i)}(z)$'s, which contradicts the linear independence assumption. This implies that each $\underline{\mathbf{s}}_i$ has at most one non-zero coefficient, which is equivalent to saying that \mathbf{S} represents the product of a permutation matrix and a diagonal matrix.

5. PRACTICAL IDENTIFICATION METHOD

The previous discussion has shown that any factorization of the form of (4) is an equally good way of decomposing $\{\underline{\mathbf{h}}_n\}$ into scalar, independent processes. Let us now derive an algorithm to find one of these decompositions. Let us assume that the noise level is known, or has been estimated, hence $S_{\underline{\mathbf{h}}\underline{\mathbf{h}}}(z)$ is known, or equivalently, $R_{\underline{\mathbf{h}}\underline{\mathbf{h}}}(u)$ is known for $u \in \mathbb{Z}$. The algorithm that we present here computes a matrix \mathbf{B} that decomposes $S_{\underline{\mathbf{h}}\underline{\mathbf{h}}}(z)$ into independent processes, *i.e.* $\mathbf{B}\mathbf{S}_{\underline{\mathbf{h}}\underline{\mathbf{h}}}(z)\mathbf{B}^H$ is diagonal. We restrict the problem to the signal subspace, and consider $\mathbf{C}^H R_{\underline{\mathbf{h}}\underline{\mathbf{h}}}(0)\mathbf{C}$. Since it is positive semi-definite, it can be decomposed according to its eigenstructure:

$$\mathbf{C}^H R_{\underline{\mathbf{h}}\underline{\mathbf{h}}}(0)\mathbf{C} = \mathbf{W}\mathbf{D}\mathbf{W}^H, \quad (13)$$

where \mathbf{W} is a $P \times P$ unitary matrix, and \mathbf{D} is diagonal, and contains the (non-negative) eigenvalues. Notice that $(\mathbf{W}\sqrt{\mathbf{D}})(\mathbf{W}\sqrt{\mathbf{D}})^H$ constitutes a Cholesky decomposition of $\mathbf{C}^H R_{\underline{\mathbf{h}}\underline{\mathbf{h}}}(0)\mathbf{C}$. Since $(\mathbf{R}\sqrt{R_{\underline{\mathbf{b}}\underline{\mathbf{b}}}(0)})(\mathbf{R}\sqrt{R_{\underline{\mathbf{b}}\underline{\mathbf{b}}}(0)})^H$ is also a Cholesky decomposition of the same matrix, they are unitarily similar [6], *i.e.* there exist an unitary matrix \mathbf{Q} s.t.

$$\left(\mathbf{R}\sqrt{R_{\underline{\mathbf{b}}\underline{\mathbf{b}}}(0)}\right)^H = \mathbf{Q}\left(\mathbf{W}\sqrt{\mathbf{D}}\right)^H. \quad (14)$$

Obviously, finding \mathbf{Q} would let us identify \mathbf{R} up to the scalar uncertainties contained in $\sqrt{R_{\underline{\mathbf{b}}\underline{\mathbf{b}}}(0)}$. In order to find

it, we use the fact that

$$\begin{aligned} & \left(\mathbf{W}\sqrt{\mathbf{D}}\right)^{-1} \mathbf{C}^H R_{\underline{\mathbf{h}}\underline{\mathbf{h}}}(u)\mathbf{C} \left(\mathbf{W}\sqrt{\mathbf{D}}\right)^{-H} \\ & = \mathbf{Q}^H R_{\underline{\mathbf{b}}\underline{\mathbf{b}}}(u)R_{\underline{\mathbf{b}}\underline{\mathbf{b}}}(0)^{-1}\mathbf{Q} \quad \forall u \in \mathbb{Z}. \end{aligned} \quad (15)$$

Under our assumptions, there is a unique way (up to a permutation \mathbf{P}) of diagonalizing the spectrum matrix, as demonstrated in section 4, hence if \mathbf{V} is a unitary matrix that diagonalizes $\mathbf{V}\sqrt{\mathbf{D}^{-1}}\mathbf{W}^H\mathbf{C}^H R_{\underline{\mathbf{h}}\underline{\mathbf{h}}}(u)\mathbf{C}\mathbf{W}\sqrt{\mathbf{D}^{-1}}\mathbf{V}^H$ for all $u \in \mathbb{Z}$, then $\mathbf{Q} = \mathbf{P}^T\mathbf{V}$. Finding \mathbf{V} is a so-called *simultaneous diagonalization* problem, and can be done numerically [7]. It follows that $\{\underline{\mathbf{h}}_n\}$ is transformed into an arbitrary vector process $\{\underline{\mathbf{y}}_n\}$, with

$$\underline{\mathbf{y}}_n \triangleq \mathbf{V}\sqrt{\mathbf{D}^{-1}}\mathbf{W}^H\mathbf{C}^H\underline{\mathbf{h}}_n = \mathbf{P}\sqrt{R_{\underline{\mathbf{b}}\underline{\mathbf{b}}}(0)^{-1}}\underline{\mathbf{b}}_n, \quad (16)$$

and $S_{\underline{\mathbf{y}}\underline{\mathbf{y}}}(z)$ is diagonal: $\mathbf{V}\sqrt{\mathbf{D}^{-1}}\mathbf{W}^H\mathbf{C}^H$ is a possible \mathbf{B} . The uncertainties outlined in section 4 appear clearly in (16): each component of $\{\underline{\mathbf{y}}_n\}$ is normalized to unitary variance, and the permutation \mathbf{P} is unknown.

Obviously, the theoretical identifiability outlined in section 4, is not realistic in practice, since implementation constraints would restrict the knowledge of $R_{\underline{\mathbf{h}}\underline{\mathbf{h}}}(u)$ to a limited range of u . Also, the requirement of linear independence of the columns of \mathbf{G} , as well as the linear independence of the z -spectrums of the time coefficients, are not guaranteed to be fulfilled in real life. However, our experiments show that these limitations do not seem to incur significant problems in practice.

6. EXPERIMENTAL RESULTS

The proposed identification method was applied to experimental data obtained from a prototype UMTS TDD link [8] operating on a 3.84MHz wide channel in the 1900-1920MHz IMT-2000 TDD band. The setting is comprised of two rooftop antennas connected to the base station, and a terminal connected to a portable antenna that was operated inside the building. The channel measurements were performed on the uplink channel, in the framework of an actual UMTS connection. The considered channel has 1 Tx and 2 Rx antennas, and the length of the observed impulse responses is $L = 36$ samples. The complete SIMO channel impulse response is estimated every 10ms using conventional channel estimation techniques, by exploiting the training sequences embedded in the UMTS traffic. The oscillators of both Rx antennas are synchronized.

\mathbf{B} is first computed by applying the proposed algorithm to a series of consecutive channel measurements, and the corresponding series $\underline{\mathbf{y}}_n$ is computed according to (16). The algorithm operates with approximate covariance matrices estimated from a finite-length measurement interval of 50

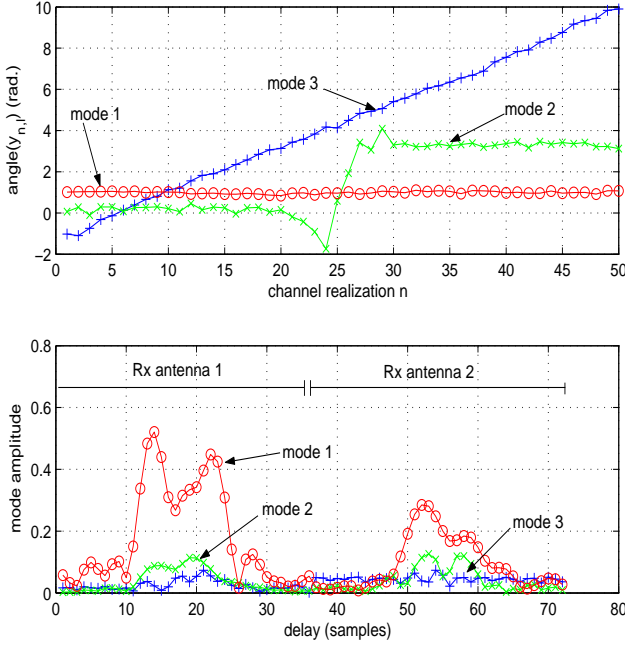


Fig. 1. Example of modal decomposition, fixed setting.

successive realizations (spanning 500ms) of $\{\mathbf{h}_n\}$. The number P' of independent random processes to track is set arbitrarily. Two series of measurements were conducted. In the first setting (fixed setting), the MT antenna lies on a table and no noticeable movement is made around the antennas. In the second setting (moving setting), the MT antenna is hand-held and moved rapidly by a human operator.

Figure 1 presents an example of the output of the algorithm for the fixed setting. The top plot represents the angles of the coefficients of \mathbf{y}_n associated with the $P' = 3$ strongest modes. The bottom plot shows the profile of the modes as identified by the algorithm (each mode corresponds to a column of $\mathbf{C}\mathbf{W}\sqrt{\mathbf{D}}\mathbf{V}^H$, the generalized inverse of \mathbf{B}). Since \mathbf{h}_n contains the impulse responses from both Rx antennas, \mathbf{B} has a similar structure, and therefore the left part of the plot represents the channel impulse response seen by the first Rx antenna, while the right part represents the channel impulse response seen by the second Rx antenna. Note that the arbitrary scaling has been partially resolved by normalizing each component of \mathbf{y}_n to unit average energy, so that the three modes can be plotted on the same scale. Figure 2 was obtained for the second series of measurements (moving setting) through the same process. In both cases, the time-varying components exhibit a high predictability. In particular, the linear phase evolution exhibited by the fixed setting can be accurately predicted by an auto-regressive (AR) model of order 1. As expected, the temporal evolution of the channel in the moving setting does

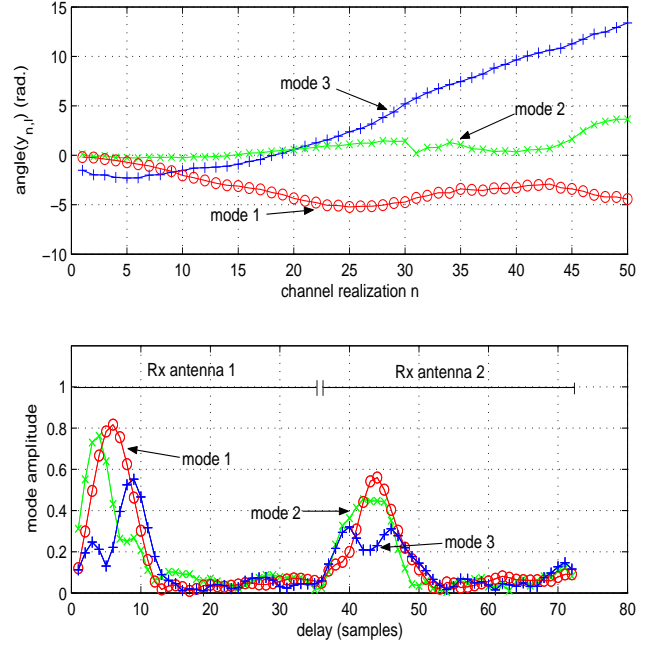


Fig. 2. Example of modal decomposition, moving setting.

not exhibit such a linear behaviour, although it could be predictable by an higher-order AR model.

It is noticeable from both figures 1 and 2 that the modes spans both Rx antennas. This indicates that the channel structure is correlated between the antennas, and that the algorithm has correctly identified a common structure in their temporal evolution. This is not contradictory with the fact that this setting provides antenna diversity, since the actual impulse responses are linear combinations (with time-varying weights) of the modes plotted here. Although the result can vary rapidly, the knowledge of the underlying structure allows for a more accurate long-term tracking.

In order to evaluate the feasibility of channel prediction, let us now present results obtained from one-step prediction applied to the time-varying coefficients. For each time instant n , after computing \mathbf{B} , the time-series corresponding to the last 50 channel realizations $\mathbf{y}_{n-49} \dots \mathbf{y}_n$ is extrapolated using an AR model. The resulting value $\hat{\mathbf{y}}_{n+1}$ is used to compute the predicted channel $\hat{\mathbf{h}}_{n+1} = \mathbf{C}\mathbf{W}\sqrt{\mathbf{D}}\mathbf{V}^H\hat{\mathbf{y}}_{n+1}$. Since the true channel value is not known, a noise metric defined as $\alpha \triangleq \mathcal{E}_n[|\tilde{\mathbf{h}}_{n+1}|^2] / \mathcal{E}_n[|\hat{\mathbf{h}}_{n+1} - \tilde{\mathbf{h}}_{n+1}|^2]$, that can be computed from the noisy channel measurements, was used. There is a saturation effect associated with this metric, since even if the prediction is perfect ($\hat{\mathbf{h}}_{n+1} = \tilde{\mathbf{h}}_{n+1}$), α goes to the input SNR. For comparison, the input SNR is 11.5dB for the fixed measurements, and 11.9dB for the moving measurements.

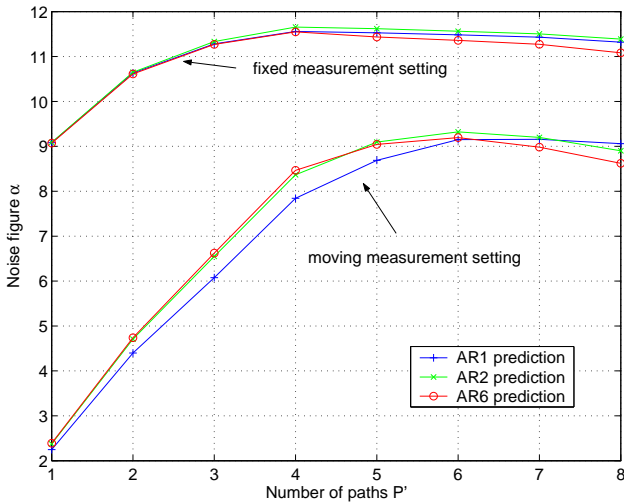


Fig. 3. Predictor noise figure α .

Figure 3 shows the evolution of α (in dB) for various orders of the AR predictor, and for various numbers of paths P' , for both sets of measurements. As expected, the channel in the fixed setting exhibits a very high predictability, and the predictor reaches the optimality ($\alpha = \text{SNR}$) for $P' = 4$ tracked paths. Increasing P' over this values slightly increases the amount of noise on the output, although for P' ranging from 3 to 8 paths, α is only a fraction of a dB from the optimality. Varying the order of the AR predictor has little influence on the performance in the fixed setting, as evidenced by the three almost superimposed curves.

This optimality is not reached for the moving setting, with α getting no closer than 2.5dB from the bound set by the SNR. The maximum accuracy is reached by tracking 6 subspaces. Note that this does not necessarily mean that 6 paths are identified, since this can be caused by the fact that the channel model can not be assumed stationary over the .5s analyzed here. The order of the AR predictor seems more critical in this case, as exemplified by the fact that the AR2 performs significantly better than the AR1, especially when P' is underestimated. This could be explained by the fact that an AR2 model can better track a mixture of AR processes than an AR1, although no definitive conclusion can be drawn at this point.

7. CONCLUSION

We presented a channel modeling method based on the assumption that the channel follows a specular structure. We showed how this structured model, by separating space and time-components, lends itself to simplified tracking, including smoothing and prediction, once the underlying space and time characteristics are separated. We proposed an identification algorithm for this structure, based on simultaneous

diagonalization of the covariance matrices. We evaluated the performance of the proposed method on experimental data, and showed that it successfully identifies the long-term channel structure of a typical UMTS wireless channel.

Acknowledgment

Eurécóm's research is partially supported by its industrial partners: Ascom, Swisscom, Thales Communications, ST Microelectronics, CEGETEL, Motorola, France Télécom, Bouygues Telecom, Hitachi Europe Ltd. and Texas Instruments.

8. REFERENCES

- [1] B.H. Fleury, P. Jourdan, and A. Stucki, "High-resolution channel parameter estimation for MIMO applications using the SAGE algorithm," in *Proc. International Zürich Seminar on Broadband Communications 2002*, Zürich, Switzerland, February 2002.
- [2] J.H. Winters and J.-K. Hwang, "Sinusoidal modeling and prediction of fast fading processes," in *Proc. IEEE Globecom '98 Conference*, 1998, vol. 2, pp. 892–897.
- [3] J.B. Andersen, J. Jensen, S.H. Jensen, and F. Frederiksen, "Prediction of future fading based on past measurements," in *Proc. IEEE Vehicular Technology Conference Fall*, 1999, vol. 1, pp. 151–155.
- [4] M. Guillaud and D. T.M. Slock, "MIMO frequency-selective channel modeling based on pathwise dynamics," in *Proc. 38th Asilomar Conference on Signals, Systems and Computers*, Pacific Grove, CA, USA, November 2004.
- [5] T. Kailath, A.H. Sayed, and B. Hassibi, *Linear Estimation*, Prentice Hall, 2000.
- [6] Roger A. Horn and Charles R. Johnson, *Matrix analysis*, Cambridge University Press, 1985.
- [7] Angelika Bunse-Gerstner, Ralph Byers, and Volker Mehrmann, "Numerical methods for simultaneous diagonalization," *SIAM Journal on Matrix Analysis and Applications*, vol. 14, no. 4, pp. 927–949, 1993.
- [8] Eurécóm Institute Mobile Communications Dept., "Activity report 2003," Tech. Rep., Eurécóm Institute, Sophia-Antipolis, France, 2003.